Coupling of Navier-Stokes Equations and Their Hydrostatic Versions for Ocean Flows: A Discussion on Algorithm and Implementation

Hansong Tang and Yingjie Liu

1 Introduction

Now it is necessary to advance our capabilities to direct simulation of many emerging problems of coastal ocean flows. Two examples of such flow problems are the 2010 Gulf of Mexico oil spill and the 2011 Japan tsunami. The two examples come from different backgrounds, however, they present a same challenge to our modeling capacity; the both examples involve distinct types of physical phenomena at vastly different scales, and they are multiscale and multiphysics flows in nature. In particular, at the bottom of ocean, the spill appeared as high-speed, three dimensional (3D) jets at scales of $O(10)$ m, whereas on the ocean surface, it became two dimensional (2D) patches of oil film at horizontal sizes of $O(100)$ km [1]. The tsunami started as surface waves with tiny amplitude in a deep ocean, then evolved into walls of water as high as 39 m near seashore, and finally impacted coastal structures such as bridges at scales of $O(10)$ m [5]. These phenomena take place at different scales, and they are better and more efficiently simulated using different governing equations and numerical methods. Currently there is lack of appropriate computational methods and corresponding computer software packages that can directly and integrally simulate those multiple physics phenomena.

A natural and most feasible approach to simulation of multiscale and multiphysics coastal ocean flows is coupling of the Navier-Stokes (NS) equations and hydrostatic versions of the Navier-Stokes (HNS) equations. In the past few decades, various computational fluid dynamics (CFD) models (i.e., computer software packages) have been built on the NS equations for fully 3D fluid dynamics at complicated,

Hansong Tang
Department of Civil Engineering, City College, City University of New York, NY 10031, USA. e-mail: htang@ccny.cuny.edu

Yingjie Liu
School of Mathematics, Georgia Institute of Technology, Atlanta, GA 30332, USA. e-mail: yingjie@math.gatech.edu

small scales ($O(1)$ cm – $O(10)$ km), such as jet flows similar to those of above oil spill [7]. At the same time, a number of CFD models have also been designed on the basis of HNS equations for geophysical fluid dynamics at large scales ($O(10)$-$O(10,000)$ km), such as the ocean currents carrying above oil patches [3]. Since the NS equations and the HNS equations are better bases for simulation of ocean flows at small and large scales, respectively, and coupling of them will enable us to conduct simulation of phenomena at larger or even full ranges of scales.

2 Governing Equations

The NS equations describe motion of flows, and they consist of the continuity equation and the momentum equation:

$$\begin{aligned} &\nabla \cdot \mathbf{u} = 0 \\ &\mathbf{u}_t + \nabla \cdot \mathbf{uu} = \nabla \cdot (\nu \nabla \mathbf{u}) - \nabla p/\rho - g\mathbf{k} \end{aligned} \tag{1}$$

Here, $\mathbf{u}$ is the velocity vector, with u and v as the components in x and y direction, respectively, on the horizontal plane, and w as the component in z direction, or, the vertical direction, $\mathbf{k}$. ν is the viscosity, ρ the density, p the pressure, and g the gravity.

HNS equations are widely used for coastal ocean flows, and they are simplified from above NS equations; with the hydrostatic assumption, only the gravity and pressure terms are kept and all others are ignored in the vertical component of the momentum equation. As a result, the governing equations of the HNS equations consist of the continuity equation and the simplified momentum equation, which read as

$$\begin{aligned} &\nabla \cdot \mathbf{u} = 0 \\ &\mathbf{v}_t + \nabla \cdot \mathbf{uv} = \nabla \cdot (\nu \nabla \mathbf{v}) - \nabla_H p/\rho \\ &p = \rho g(\eta - z) \end{aligned} \tag{2}$$

where $\mathbf{v} = (u, v)$, η is the elevation of water surface, and ∇_H is the gradient in the horizontal plane.

In view of the third equation for pressure in (2), its momentum equation in the horizontal plane can be rewritten as

$$\mathbf{v}_t + \nabla \cdot \mathbf{uv} = \nabla \cdot (\nu \nabla \mathbf{u}) - g \nabla_H \eta \tag{3}$$

Additionally, by pressure splitting $p = p_d + \rho g(\eta - z)$, where p_d is the dynamic pressure, the momentum equation in (1) becomes

$$\mathbf{u}_t + \nabla \cdot \mathbf{uu} = \nabla \cdot (\nu \nabla \mathbf{u}) - \nabla p_d/\rho - g \nabla_H \eta \tag{4}$$

3 Computational Methods

3.1 Transmision Condition

Let a flow field ω be divided into subdomains of NS and HNS by their interface γ, as shown in Fig. 1. Consider the weak solution of the continuity equation in (1) and (2) that satisfies

$$\int_{\omega} \mathbf{u} \cdot \nabla \phi d\omega = 0 \tag{5}$$

for any $\phi \in C_0^{\infty}$. Let ω be an arbitrarily selected a region across the interface, and $\omega = \omega_1 \cup \omega_2$, with ω_1 and ω_2 falling in the regions of NS and HNS, respectively (Fig. 1). In view that

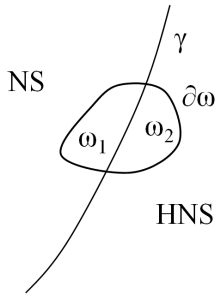

Fig. 1: Division of a flow region into a NS region abd a HNS region.

$$\int_{\omega} \mathbf{u} \cdot \nabla \phi d\omega = \int_{\gamma} \phi(\mathbf{u}_n|_{\gamma_-} - \mathbf{u}_n|_{\gamma_+}) d\omega - \int_{\omega_1 \cup \omega_2} \phi \nabla \cdot \mathbf{u} d\omega \tag{6}$$

it is readily seen that, under the divergence-free condition (i.e., the first equation in (1) or (2)), continuity of normal velocity across the interface

$$\mathbf{u}_n|_{\gamma_-} = \mathbf{u}_n|_{\gamma_+} \tag{7}$$

is a sufficient and necessary condition for $\mathbf{u}$ to be a weak solution. Here n means the normal direction of γ pointing from ω_1 to ω_2, $\mathbf{u}_n = \mathbf{u} \cdot \mathbf{n}$, and γ_- and γ_+ indicate the ω_1- and ω_2-side of interface γ, respectively. Therefore, condition (7) can be a transmission condition.

Similar analysis may be made for the momentum equations in the horizontal plane in (1) and (2), and it leads to the following transmission condition:

$$(\mathbf{u}_n \mathbf{v} + p_{n'}/\rho - \nu \partial \mathbf{v}/\partial n)_{\gamma_-} = (\mathbf{u}_n \mathbf{v} + p_{n'}/\rho - \nu \partial \mathbf{v}/\partial n)_{\gamma_+} \tag{8}$$

here n' refers to the normal direction, pointing from ω_1 to ω_2, of the interface's projection onto the horizontal plane. It is noted that since p is a scalar, $p_{n'}$ may be replaced by p in (8). Also, a condition similar to (8) has been proposed in [2]. In correspondence to Eqs. (3) and (4) and also in view that surface elevation can be determined by HNS equations (see discussion in Sect. 4), its values on γ_- and γ_+ cancel each other as long as the elevation is continuous across the interface. As a result, interface condition (8) becomes

$$\left(\mathbf{u}_n\mathbf{v} + p_{dn'}/\rho - \nu\partial\mathbf{v}/\partial n\right)_{\gamma_-} = \left(\mathbf{u}_n\mathbf{v} - \nu\partial\mathbf{v}/\partial n\right)_{\gamma_+} \tag{9}$$

where, for a similar reason, $p_{dn'}$ may be replaced by p_d, and its value is zero in the hydrostatic region.

It is noted that, instead of those described as above, different interface conditions may be used:

$$\mathbf{u}|_{\gamma_-} = \mathbf{u}|_{\gamma_+},\ \partial p_d/\partial n|_{\gamma_-} = 0. \tag{10}$$

Here, the continuity of whole velocity is required across the interface. Interface condition (10) is commonly used to solve NS equations, and it has been used in coupling of NS and HNS equations, see Sect. 4.

3.2 Schwarz Iteration

Let discretization of NS equations and HNS equations be written as

$$\mathbf{F}(\mathbf{f}) = \mathbf{0},\ \ \mathbf{H}(\mathbf{h}) = \mathbf{0}, \tag{11}$$

in which $\mathbf{f} = (\mathbf{u}, p_d)$, and $\mathbf{h} = (\mathbf{u}, \eta)$, with the former and the latter being the solution for NS and HNS, respectively. Since the discretization is nonlinear, an iteration within each of the two equations in (11), named as the internal iteration, is needed for their solutions. Also, because the two equations in (11) are coupled with each other, another iteration between them, referred to as the external iteration, is also necessary.

From time level n to $n+1$, a Schwartz waveform relaxation approach is used to compute the discretization and exchange solution at the interfaces:

$$\begin{array}{l}
\bar{\mathbf{f}}^{0,K_1} = \mathbf{f}^n,\ \bar{\mathbf{h}}^{0,K_2} = \mathbf{h}^n \\
Do\ 1\ m = 1, M \\
\qquad \begin{cases} \mathbf{F}(\bar{\mathbf{f}}^{m,k_1}) = \mathbf{0}, & \\ k_1 = 1, 2, \ldots, K_1, & \mathbf{x} \in \omega_1 \\ \bar{\mathbf{f}}^{m,k_1} = \hat{\mathbf{f}}^m, & \mathbf{x} \in \gamma_1 \end{cases} \qquad \begin{cases} \mathbf{H}(\bar{\mathbf{h}}^{m,k_2}) = \mathbf{0}, & \\ k_2 = 1, 2, \ldots, K_2, & \mathbf{x} \in \omega_2 \\ \bar{\mathbf{h}}^{m,k_2} = \hat{\mathbf{h}}^m, & \mathbf{x} \in \gamma_2 \end{cases} \\
1\ End\ Do \\
\mathbf{f}^{n+1} = \bar{\mathbf{f}}^{M,K_1},\ \bar{\mathbf{h}}^{n+1} = \bar{\mathbf{h}}^{M,K_2}
\end{array} \tag{12}$$

in which $\hat{\mathbf{f}}^m = \kappa_1(\bar{\mathbf{h}}^{m-1,K_2})$, $\hat{\mathbf{h}}^m = \kappa_2(\bar{\mathbf{f}}^{m-1,K_1})$, being operators for solution exchange between NS and HNS equations on their interfaces γ_1 and γ_2, respectively (γ_1 and γ_2 overlap when the subdomains of NS and HNS patch with each other). M is a prescribed external iteration number, and K_1 and K_2 are prescribed internal iteration numbers.

An issue is how to compute (12) efficiently. A possible approach to speed up its convergence is to introduce relaxation to solution exchange at the interfaces, or, to the external iteration:

$$\begin{aligned} \bar{\mathbf{f}}^{m,k_1} &= \hat{\mathbf{f}}^{m-1} + \alpha(\hat{\mathbf{f}}^{m} - \hat{\mathbf{f}}^{m-1}), \quad \mathbf{x} \in \gamma_1 \\ \bar{\mathbf{h}}^{m,k_2} &= \hat{\mathbf{h}}^{m-1} + \alpha(\hat{\mathbf{h}}^{m} - \hat{\mathbf{h}}^{m-1}), \ \mathbf{x} \in \gamma_2 \end{aligned} \tag{13}$$

As $\alpha < 1$ and > 1, the iteration "under-relaxation" and "over-relaxation", respectively. An optimal value for α may be determined as the one that leads to a quick reduction of the residual of Eq. (11). For instance, let

$$Q(\mathbf{f}, \mathbf{h}) = \langle \mathbf{F}, \mathbf{F} \rangle + \langle \mathbf{H}, \mathbf{H} \rangle \geq 0 \tag{14}$$

By Taylor expansion and Eq. (13), one has

$$\begin{aligned} & Q(\bar{\mathbf{f}}^{m,K_1}, \bar{\mathbf{h}}^{m,K_2}) \\ &= Q(\bar{\mathbf{f}}^{m-1,K_1}, \bar{\mathbf{h}}^{m-1,K_2}) \\ &+ \langle \partial Q/\partial \mathbf{f}|^m (\bar{\mathbf{f}}^{m,K_1} - \bar{\mathbf{f}}^{m-1,K_1}) \rangle_{\omega_1 \setminus \gamma_1} + \langle \partial Q/\partial \mathbf{h}|^m (\bar{\mathbf{h}}^{m,K_2} - \bar{\mathbf{h}}^{m-1,K_2}) \rangle_{\omega_2 \setminus \gamma_2} \\ &+ \alpha \left(\langle \partial Q/\partial \mathbf{f}|^m (\hat{\mathbf{f}}^{m} - \hat{\mathbf{f}}^{m-1}) \rangle_{\gamma_1} + \langle \partial Q/\partial \mathbf{h}|^m (\hat{\mathbf{h}}^{m} - \hat{\mathbf{h}}^{m-1}) \rangle_{\gamma_2} \right) \\ &+ \alpha^2 (\cdots) + \cdots \end{aligned} \tag{15}$$

An expression for an optimal α can be derived from above equation by, say, letting $Q(\bar{\mathbf{f}}^{m,K_1}, \bar{\mathbf{h}}^{m,K_2}) = 0$ or $\partial Q/\partial \alpha = 0$, hoping that $\bar{\mathbf{f}}^{m,K_1}$ and $\bar{\mathbf{h}}^{m,K_2}$ are the fixed point of the iteration. It is noted that in pursuing above iteration with relaxation, it may be important to enforce the divergence-free condition.

Another approach to speed up the convergence in computation of (12) is via an optimal combination of the internal and external iterations. A natural arrangement of them is that the external iteration marches forwards only after the internal iterations converge, i.e., at sufficiently large K_1 and K_2. However, it is expected that an optimal combination of K_1 and K_2 is possible in terms of fast convergence to solutions at time level $n + 1$. With such an optimal combination, a new external iteration may start before the full convergence of the two internal iterations, and this could be an interesting topic.

4 Implementation of Model Coupling

The Solver of Incompressible Flow on Overset Meshes (SIFOM) is developed to compute NS equations (e.g., [6]), and its governing equations are

$$\begin{aligned} & \nabla \cdot \mathbf{u} = 0 \\ & \mathbf{u}_t + \nabla \cdot \mathbf{u}\mathbf{u} = \nabla \cdot ((\nu + \nu_t) \nabla \mathbf{u}) - \nabla p'_d/\rho - g \nabla_H \eta \end{aligned} \tag{16}$$

in which ν_t is the turbulence viscosity. SIFOM discretizes above equations in curvilinear coordinates using a finite difference method [6].

An HNS solver is the Finite Volume Method Coastal Ocean Model (FVCOM), and its hydrostatic version consists of an external and an internal mode [4]. The governing equations for the external mode are the vertically averaged continuity and momentum equations:

$$\begin{aligned} &\eta_t + \nabla_H \cdot (\mathbf{V}D) = 0 \\ &(\mathbf{V}D)_t + \nabla_H \cdot (\mathbf{V}\mathbf{V}D) = -gD\,\nabla_H\,\eta + (\tau_s - \tau_b)/\rho + \mathbf{E}. \end{aligned} \tag{17}$$

The governing equations of the internal mode are the 3D continuity and momentum equations associated with the hydrostatic assumption:

$$\begin{aligned} &\eta_t + \nabla_H \cdot (\mathbf{v}D) + \omega_\sigma = 0, \\ &(\mathbf{v}D)_t + \nabla_H \cdot (\mathbf{v}\mathbf{v}D) + (\mathbf{v}\omega)_\sigma = -gD\,\nabla_H\,\eta + \nabla_H \cdot (\kappa\mathbf{e}) \\ &\qquad\qquad + (\lambda\mathbf{v}_\sigma)_\sigma/D + \mathbf{I}, \end{aligned} \tag{18}$$

In the external mode, $\mathbf{V}$ is the depth-averaged velocity vector, D is the water depth, and τ_s and τ_b are the shear stress on water surface and seabed, respectively. $\mathbf{E}$ includes the other terms such as the Coriolis force. In the internal mode, σ is the vertical coordinate, ω the vertical velocity in the σ-coordinate, $\mathbf{e}$ the strain rate, subscript σ the derivative over σ, and $\mathbf{I}$ the other terms. κ, and λ are coefficients. FVCOM solves Eqs. (17) and (18) on a triangular grid in the horizontal plane and a σ-grid in the vertical direction using a finite volume method.

An approach to integrate SIFOM and FVCOM is to couple Eqs. (16) and (18). The integration follows the algorithm (12). Interface transmission condition (10) is used for both SIFOM and FVCOM at their interfaces. It is noted that water surface elevation in SIFOM, or Eq. (16), is computed by FVCOM, or Eq. (17). Also, SIFOM and FVCOM are models for complicated, realistic flow problems, and their governing equations are not exactly but approximately same to the NS and HNS equations, respectively. For instance, Eq. (18) is a form transformed from Eq. (2). More details on the interface treatments and numerical algorithms can be found in [8].

As an example on performance of the SIFOM-FVCOM system, simulation has been made for a flow over a sill in a channel, see Fig. 2. In the simulation, SIFOM occupies the contraction section of the channel, and FVCOM covers all the channel, except a blanked region within the zone of SIFOM. Here, two regions for the SIFOM's are used; one is bigger and the other is smaller, and they lead to different interface locations. In the figure, it is seen that the simulated flow passes the interfaces of SIFOM smoothly, and no obvious artifact is generated there. However, the simulations with the two SIFOM regions present certain difference; as illustrated by streamlines, the simulation with the larger region presents more vibrating vertical motion after the contraction section, which is anticipated because SIFOM permits strong vertical motion. More simulated results for the flow are available in [8, 9], and they show that solution presents patterns similar to that by SIFOM alone, e.g., the vortical structures after the contraction section, and this is an intention of the coupling approach.

Simulation of actual ocean flows is challenging. For instance, as seen in Fig. 2, the simulated solution with a bigger SIFOM region is somewhat different from that with

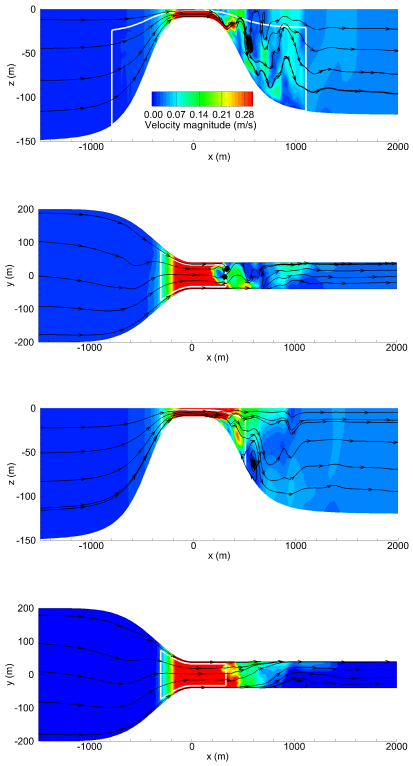

Fig. 2: Simulated instantaneous solutions of the sill flow. The solid white lines are SIFOM's interfaces, The top two panels have a bigger SIFOM region, and the bottom two panels have a smaller SIFOM region. In each set of the two panels, the first one is a side view, and the second one is a top view. In this simulation, to make it simple, M is set as 1, or, no iteration is made between SIFOM and FVCOM.

a smaller SIFOM region, indicating the influence of the size of the SIFOM's region and locations of the interfaces. Moreover, since it involves multiple times of runs of both SIFOM and FVCOM in marching from time level n to $n+1$, Schwarz iteration (12) is expensive, and it is significant to speed up the iteration. For this purpose, a preliminary effort has been made by running the SIFOM-FVCOM system with a few prescribed values for α in Eq. (13). However, no obvious speedup in convergence has been achieved, and this indicates that a deliberate design for the value of α is necessary.

Finally, it is noted that, in a recent study, another solver for the NS equations and implemented with a volume of fraction method has been coupled to FVCOM using techniques similar to those of the SIFOM-FVCOM system, and the results are encouraging [10].

5 Concluding Remarks

An successful coupling of NS and HNS equations will lead to an avenue to simulation of multiscale and multiphysics in many emerging coastal ocean flow problems. This paper presents a preliminary study on such coupling with regard to transmission conditions, Schwartz iterations, and coupling of actual models. In view that it is a relatively new topic and its realization is complicated, the coupling deserves systematic theoretical analysis and numerical experimentation, and we shall keep what discussed in this paper, in particular, the transmission conditions and the Schwarz iterations, for future study, and explore their effectiveness.

Acknowledgements This work is supported by the NSF (DMS-1622453, DMS-1622459). The example simulation in Fig. 2 is made by Mr. Wenbin Dong.

References

1. BBC.: Gulf of Mexico oil leak 'worst US environment disaster'. May 30, 2010 http://www.bbc.co.uk/news/10194335.
2. Blayo, E. and Rousseau, A.: About interface conditions for coupling hydrostatic and nonhydrostatic navier-stokes flows. Discrete and Continuous Dynamical Systems Series. **9**, 1565-1574 (2016).
3. Blumberg, A.F. and Mellor, G. L.: A description of a three-dimensional coastal ocean circulation model, in Three-Dimensional Coastal Models, Coastal Estuarine Ser., vol. 3, edited by N. S. Heaps, 1 – 16, AGU, Washington, D. C, 1987.
4. Chen, C. and Liu, H. and Beardsley, R.C.: An unstructured, finite-volume, three-dimensional, primitive equation ocean model: application to coastal ocean and estuaries. J. Atm. & Oceanic Tech. **20**, 159-186(2003).
5. Mimura, N. and Yasuhara, K. and Kawagoe, S. and Yokoki, H. and Kazama, S.: Damage from the great east japan earthquake and tsunami - a quick report. Mitig. Adapt. Strateg. Glob. Change. **16**, 803 – 818 (2011)
6. Tang, H.S. and Jones, S.C. and Sotiropoulos, F.: An overset-grid method for 3D unsteady incompressible flows. J. Comput. Phys. **191**, 567-600 (2003).
7. Tang, H.S. and Paik, J. and Sotiropoulos, F. and Khangaokar, T.: Three-dimensional numerical modeling of initial mixing of thermal discharges at real-life configurations. ASCE J. Hydr. Eng. **134**, 1210 – 1224 (2008)
8. Tang, H.S. and Qu, K. and Wu, X.G.: An overset grid method for integration of fully 3D fluid dynamics and geophysical fluid dynamics models to simulate multiphysics coastal ocean flows. J. Comput. Phys. **273**, 548 – 571 (2014).
9. Tang, H.S. and Qu, K. and Wu, X.G. and Zhang, Z.K.: Domain decomposition for a hybrid fully 3D fluid dynamics and geophysical fluid dynamics modeling system: A numerical experiment on a transient sill flow. Domain Decomposition Methods in Science and Engineering XXII, 407-414. Ed: Dickopf, T. and Gander, M.J. and Halpern, L. and Krause, R. and Pavarino, L.F. Springer, 2016.
10. Qu, K. and Tang, H. S. and Agrawal, A.: Integration of fully 3D fluid dynamics and geophysical fluid dynamics models for multiphysics coastal ocean flows: Simulation of local complex free-surface phenomena, Ocean Modelling, **135**, 14 –30 (2019).